



OPEN

Characterising particulate matter source contributions in the pollution control zone of mining and related industries using bivariate statistical techniques

Sirapong Sooktawee¹, Thongchai Kanabkaew^{2,3✉}, Suteera Boonyapitak¹,
Aduldech Patpai¹ & Nirun Piemyai¹

Na Phra Lan Subdistrict is a pollution control zone with the highest PM₁₀ level in Thailand. Major mobile and industrial sources in the area are related to stone crushing, quarrying and mining. This study used statistical techniques to investigate the potential sources influencing high PM₁₀ levels in Na Phra Lan. Hourly PM₁₀ data and related parameters (PM_{2.5}, PM_{coarse} and NO_x) from 2014–2017 were analysed using time series, bivariate polar plot and conditional bivariate probability function (CBPF). Results of diurnal variation revealed two peaks of PM₁₀ levels from 06:00–10:00 and 19:00–23:00 every month. For seasonal variation, high PM₁₀ concentrations were found from October to February associated with the cool and dry weather during these months. The bivariate polar plot and CBPF confirmed two potential sources, i.e., resuspended dust from mobile sources close to the air quality monitoring station (receptor) and industrial sources of mining, quarrying and stone crushing far from the station on the northeast side. While the industrial source areas played a role in background PM₁₀ concentrations, the influence of mobile sources increased the concentrations resulting in two PM₁₀ peaks daily. From the study results, we proposed that countermeasure activities should focus on potential source areas, resuspended road dust from vehicles and the industrial sources related to quarrying and mining, rather than distributing equal attention to all sources.

Particulate matter (PM) in the air is an important issue for sustainable development. The United Nations anticipates achieving the Sustainable Development Goals (SDGs) by 2030. Annual mean levels of PM_{2.5} and PM₁₀ are indicators of goal 11 of the SDGs that aims to make cities and human settlements inclusive, safe, resilient and sustainable¹. The recommended PM₁₀ values from the guidelines of the World Health Organisation (WHO) are 50 and 20 µg/m³ for 24-h and annual averages, respectively². Exposure to high level of PM causes several adverse health problems both acute and chronic effects, e.g., bronchitis, asthma, respiratory and cardiovascular diseases^{3–5}, and diabetes⁶ that subsequently induce the years of human life lost⁷. Regarding populations in developing countries, around 9 of 10 individuals were found to have a high possibility of being exposed to higher levels of PM than those specified in WHO guidelines⁸. Recently, Taneepanichskul et al.⁹ found an increased risk of mortality in 12 provinces of Thailand attributable to increased PM₁₀ concentrations, particularly during the winter months (November to February).

For Thailand, the PM₁₀ levels in Na Phra Lan Subdistrict, Saraburi Province, have reached the highest in the country for a few decades¹⁰. Since 1997, air quality monitoring station has measured PM₁₀ concentration in the area. The maximum 24-h average in 1997 was 693 µg/m³ and 37% of observed times (54 of 147) exceeded the National Ambient Air Quality Standard (NAAQS), i.e., 120 µg/m³ for 24-h average as posted in the <http://air4t>

¹Environmental Research and Training Center, Department of Environmental Quality Promotion, Ministry of Natural Resources and Environment, Pathumthani, Thailand. ²Department of Sanitary Engineering, Faculty of Public Health, Mahidol University, Bangkok, Thailand. ³Center of Excellence on Environmental Health and Toxicology, Bangkok, Thailand. ✉email: thongchai.kaa@mahidol.ac.th

hai.pcd.go.th website of the Pollution Control Department (PCD) of Thailand. Therefore, the Thai government has designated Na Phra Lan Subdistrict as a “Pollution Control Zone” since 2004 and the local governor was given the authority to implement specific action plans to mitigate the problem¹¹. From 2012 to present, the tendency of PM₁₀ concentrations in other parts of the country revealed a decreasing trend, except for the area of Na Phra Lan Subdistrict¹⁰.

The PM₁₀ sources in Na Phra Lan Subdistrict were observed to be mainly from industrial processes related to quarrying activities such as mineral processing plants, crushed stone plants, and stone mines^{12–14}. Nonetheless, not only were the industrial sources, but also the resuspended road dust from transporting mining products identified as major sources of PM₁₀¹⁴. Related studies using the source dispersion model have indicated that PM₁₀ levels at receptors were generated mainly from line source emissions of resuspended road dust, followed by area sources related to mining industries^{13,14}. However, dispersion model utilised estimated emission sources and simulated meteorological parameters. Various assumptions of emission estimation have been applied to specify activity data, emission factors, and temporal and spatial allocations of emission inputs that could create uncertainties in the prediction. Simulated meteorological parameters were also downscaled and processed using a large-scale meteorological input from reanalysed datasets with 1 × 1° resolution from the National Center for Environmental Prediction. High variable meteorological parameters such as wind speed and wind direction from model simulation were seen to be not in good agreement with the observation. In addition, a selected episode of short period for model simulation as 2 days of HYPACT in winter and rainy seasons¹³, and normally a 1-year basis of AERMOD run without model result evaluation with the reference monitoring data¹⁴ could pose a level of uncertainties. In addition, no relationship among temporal variations of PM₁₀, meteorological parameters, and emission source contribution and locations has been clearly described in Na Phra Lan area. Other studies have also reported that the dispersion model result did not provide adequate information of locations and directions of source contributions to the receptors regarding specific temporal variation and, to some extent, the incomplete information of the sources and their emissions was regarded as the model limitation^{15,16}. Therefore, this study aimed to provide further information to characterise PM₁₀ source contributions, their diurnal emissions and their locations, using integrated statistical techniques: bivariate polar plot and conditional bivariate probability function (CBPF) for long-term actual monitoring data from 2014–2017. Results are anticipated to be useful to policymakers to appropriately reduce PM₁₀ from the accurate and potential sources in the Na Phra Lan pollution control zone.

Statistical techniques using bivariate polar plot and CBPF provide benefits to identify source characterisation in a complex emission area and display filtering air pollution data associated with wind speed and direction, and time of day; hence, they provide directionality of sources in a specific time period^{15,17–19}. CBPF has proven to be useful to identify the direction of major emission sources in rural New York State, US from December 2004 to December 2008²⁰. Uria-Tellaetxe and Carslaw¹⁵ conducted their study in the North Lincolnshire Unitary Area, UK reporting that CBPF was an effective tool to detect source direction of NO_x and SO₂ while bivariate polar plot provided information on source dispersion. Combining these statistical techniques with the area map, the specific sources of emissions could then be identified¹⁵. In addition, the bivariate polar plot and CBPF were used as effective tools to assess and manage air quality in various regions including Belgrade, Serbia²¹, Lahore, Pakistan²² and 16 cities in south central Chile²³.

Study area and methods

Na Phra Lan Subdistrict is a part of Chaloe Phra Kiat District, Saraburi Province located in central Thailand. This subdistrict accommodates various activities related to PM₁₀ emission, e.g., mining, quarrying, and stone crushing. The Department of Primary Industries and Mines reported on the website, <http://www1.dpim.go.th>, that 33 stone crushing plants were located in Na Phra Lan Subdistrict of 53 plants in Saraburi Province, and 7 limestone concessions in Na Phra Lan Subdistrict of 20 concessions in the province. The PCD reported that the maximum 24 h average concentration of PM₁₀ was 268 µg/m³ from 2014–2017 whereas the 24-h average NAAQS of PM₁₀ was 120 µg/m³. In terms of interannual variation, the annual average PM₁₀ was around 100 µg/m³, and higher than the annual NAAQS of PM₁₀ (50 µg/m³). The air quality monitoring station operated by PCD is located in the area of Na Phra Lan police station close to the main road, Pahonyothin Road. A map in Fig. 1 presents the location of the air quality station and Na Phra Lan Subdistrict. Hourly PM₁₀, PM_{2.5}, NO_x, wind speed and direction, rain and relative humidity (RH) data from 2014–2017 were observed at this station and used for analysis. Thermo Scientific Model 5014i Beta Continuous Particulate Monitor unit has been used to measure PM₁₀ and PM_{2.5}, and the 42i model has been utilised for NO_x monitoring. For wind speed and direction, rain and RH monitoring, LSI LASTEM instruments have been used. The observed hourly missing data were 2.8%, 32.7%, and 6.9% for PM₁₀, PM_{2.5}, and NO_x, respectively. The PM_{2.5} data has been checked that its magnitude should not be greater than PM₁₀. The hourly PM_{coarse} was calculated by subtracting the corresponding hourly PM_{2.5} from PM₁₀ concentrations.

Data were analysed to visualise the historic variations in PM₁₀ concentrations and potential source contributions to understand the air quality situation within the study area. R program²⁴ with OpenAir package²⁵ was used and the analysis was divided into two main parts. The first part comprised temporal analysis to understand the situation and variation of PM₁₀ levels in the study area by examining wind rose, pollution rose, intra-annual variation, and diurnal variation. The second part was analysed using the bivariate polar plot and CBPF to examine the spatial analysis, and identify potential emission sources of PM₁₀ contributing to air quality in Na Phra Lan; hence, the monitoring station was used as a receptor point for the study.

Bivariate polar plot is a technique for producing statistical values such as mean value in the polar pattern with radial (r) and angles (θ). For air quality analysis, radial axis (r) and angular axis (θ) were used to represent wind speed and wind direction, respectively. Wind speed and wind direction were divided into small cells. Then, PM₁₀

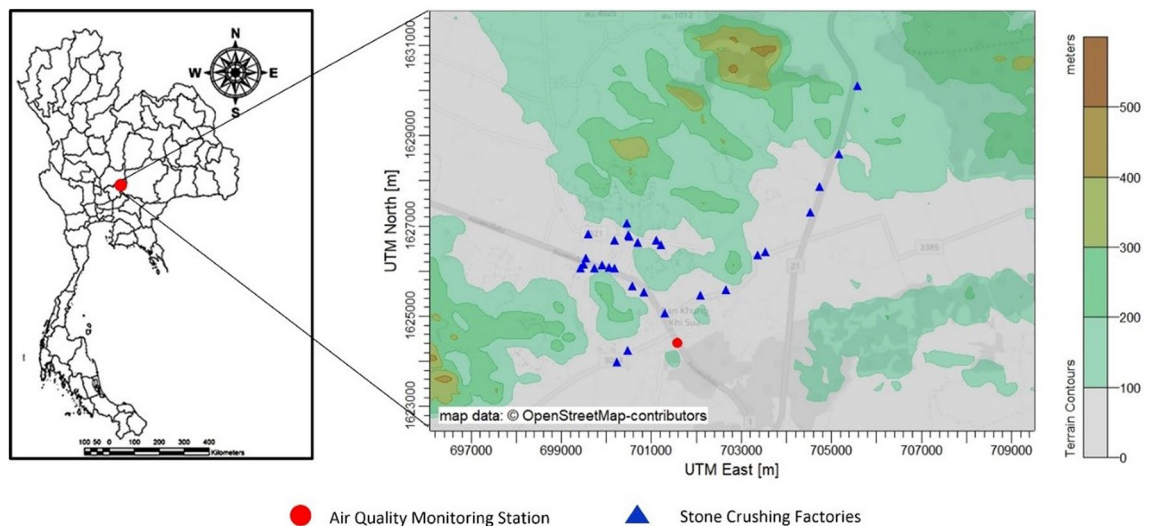


Figure 1. Study area and the location of air quality monitoring station located in Na Phra Lan Subdistrict (a map was created using AERMOD View 9.8.1, www.weblakes.com/products/aermod/).

concentration data were distributed into a related cell of wind speed and wind direction. The statistical metrics such as mean value of PM_{10} were calculated and shaded in that corresponded cell of the polar coordinate. The shading surface was smooth with general auxiliary models (GAM) indicated in Eq. (1) as follows:

$$\sqrt{C_i} = \beta_0 + s(u_i, v_i) + \varepsilon_i \quad (1)$$

where, C_i is the pollutant concentration, β_0 is overall mean of response, $s(u_i, v_i)$ is the smooth function, u and v are the wind components: $u = \bar{u} \cdot \sin(2\pi/\theta)$ and $v = \bar{u} \cdot \cos(2\pi/\theta)$, \bar{u} is the mean wind speed, ε_i is residual¹⁵. This technique can be used to determine the potential source of air pollutants such as identify the potential source of various pollutants at the Scunthorpe Town, U.K.¹⁵, and at Krakow, Poland²⁶.

For CBPF, this technique is based on the probability of the observed pollutant concentrations that exceed the threshold set for each range of wind speed and wind direction. CBPF value in each range of threshold concentrations can identify the potential emission sources of pollution that affect the monitoring point¹⁵. However, CBPF is a receptor model, and its results cannot be used to directly compare with the measurement value which is different from the results given by the source dispersion model²⁷. The result obtained from CBPF analysis can be used to compare with a spatial map to determine the consistency of the significant source influencing the level of pollutant at air quality monitoring station^{15,22}. CBPF can be calculated using Eq. (2) as follows:

$$CBPF_{\Delta\theta, \Delta v} = \frac{m_{\Delta\theta, \Delta v} |_{y \geq C \geq x}}{n_{\Delta\theta, \Delta v}} \quad (2)$$

where, $m_{\Delta\theta, \Delta v}$ is a number of sampling data with concentration between the given concentration interval x and y , and within the range of wind speed (Δv) and wind direction ($\Delta\theta$). $n_{\Delta\theta, \Delta v}$ is a number of sampling data with any concentrations within the range of wind speed (Δv) and wind direction ($\Delta\theta$)¹⁵.

Results and discussion

Situation of PM_{10} in Na Phra Lan subdistrict. To understand the mechanisms that enhance high PM_{10} concentrations in Na Phra Lan Subdistrict, intra-annual variations of PM_{10} were visualised using monthly average analysis. The intra-annual variation revealed that PM_{10} and $PM_{2.5}$ concentrations were higher than the Thailand NAAQS from approximately October to February, and January to February, respectively (Fig. 2). Both $PM_{2.5}$ and PM_{10} were also over the interim target-2 level of WHO air quality guideline for PM: 24-h concentrations, which are 100 and 50 $\mu\text{g}/\text{m}^3$ for PM_{10} and $PM_{2.5}$, respectively². Variation of the PM changes in relation to seasons; PM becomes high when amount of rain is less, and vice versa for high intensity of rain. The season changes from rainy to winter in late October. The latter season from November to February becomes the dominant mode of weather governing climatic conditions over Thailand and among its neighbours^{28,29}. During winter season, the Siberian High is a dominant forcing that results in changes of pressure gradient, temperature, precipitation, wind circulation, and others over Thailand^{28,30}. In addition, planetary boundary layer (PBL) is another factor in wintertime affecting air quality. PBL over terrestrial area located in tropical zone of the northern hemisphere becomes lower than other seasons³¹. The height of PBL that performs complete mix of substances emitted into the layer has been known as the mixing height, and is determined by pinpointing the temperature inversion on the vertical temperature profile³². Cold air traveling during winter season causes the PBL depth to become shallow resulting in reduction of the mixing height^{31,32}, which relates to reduction of air volume utilised for mixing substances and results in an increase of air pollutant concentration if the pollutant mass is constant.

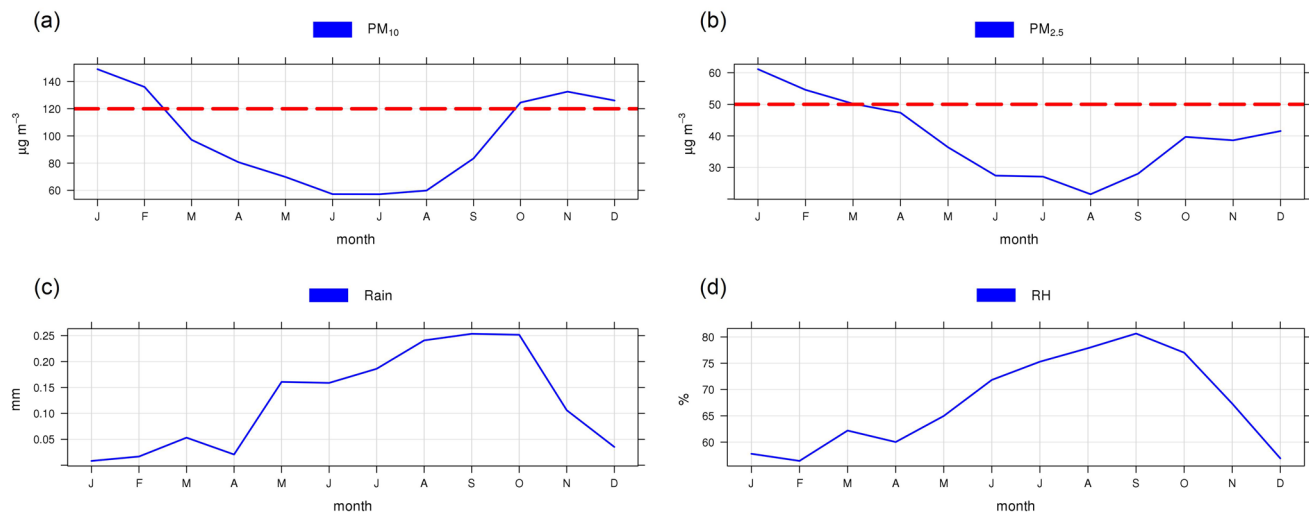


Figure 2. Intra-annual variations of (a) PM_{10} , (b) $PM_{2.5}$, (c) rain, and (d) RH (relative humidity) (the dash line is the 24-h NAAQS of PM_{10} and $PM_{2.5}$).

There is a large amount of precipitation and high RH during the wet period (May to October) caused by the summer monsoon^{30,33}. Air pollutants are removed by atmospheric processes such as wash-out and less photochemical reactions during rainfall enhancing reduction of PM_{10} , $PM_{2.5}$, and gaseous pollutants³⁴. We can conclude that intra-annual variations of PM_{10} and $PM_{2.5}$ relate mainly to climatic variation. The PM_{10} and $PM_{2.5}$ concentrations at Na Phra Lan Subdistrict increase during winter season under the strong atmospheric inversion associated with cool air mass and high pressure. Furthermore, seasonal variation does not only result in a change of climatic scalar parameters but also affects a change of wind that is a vector parameter.

During winter, wind circulation over Thailand is governed by the northeasterly wind²⁸. This particular meteorological condition is one of the factors resulting in the change of pollution concentrations and plays an important role in leveling up the pollution in the country^{35–37}. Wind rose and pollution rose were constructed using data from the air quality monitoring station to investigate associations between the wind and PM_{10} at the receptor. Results revealed that approximately 70% of wind data were mainly from the direction between northeast and southwest (Fig. 3a). The low frequency of northwesterly wind is due to the elevated terrain located at the northern and western areas of the station (see Fig. 1), and it is not the prevailing wind direction of summer and winter monsoons. When considering the pollution rose (Fig. 3b,c), PM_{10} and $PM_{2.5}$ levels, higher than 100 and 50 $\mu\text{g}/\text{m}^3$, were mainly from the east side of the air quality station (from northeast to southeast). Figure 3d shows the pollution rose of PM_{coarse} , which is a main ingredient of PM_{10} . High PM_{coarse} concentrations were mainly from northeast to southeast direction, and similar to the PM_{10} . Therefore, it is interesting to investigate the $PM_{2.5}/PM_{10}$ ratio further because the ratio could help suggest types of PM sources³⁸.

Separated monthly pollution rose plots were then investigated in Fig. 4 to scrutinise the effects of meteorological patterns on the pollution formation. The proportion of high PM_{10} concentrations was presented from October to February with the predominant winds from the direction between northeast and southeast consistent with the overriding winter monsoon. However, with the wind blowing from other directions in other months, the proportion of high PM_{10} concentrations was significantly lower than in winter. The pollution roses suggest that significant PM_{10} sources would be located at the east area during the winter season. Pollution roses of PM_{coarse} were similar to those of PM_{10} in terms of frequency with slightly lower concentrations whereas for $PM_{2.5}$ roses, concentrations were significantly lower than PM_{10} (Figures S1 and S2 in supplementary).

Mean concentrations of PM_{10} , $PM_{2.5}$, PM_{coarse} , and NO_x in Na Phra Lan Subdistrict were 97.98 $\mu\text{g}/\text{m}^3$, 39.37 $\mu\text{g}/\text{m}^3$, 65.84 $\mu\text{g}/\text{m}^3$, and 53.71 ppb, respectively. The mean $PM_{2.5}/PM_{10}$ ratio was 0.4 and the correlation of PM_{10} and PM_{coarse} was 0.95, whereas that of PM_{10} and $PM_{2.5}$ was 0.67 at 99 percent confidence level. This revealed that the PM_{10} level in Na Phra Lan Subdistrict would be contributed by PM_{coarse} more than $PM_{2.5}$. The correlations of NO_x and PM_{10} , and $PM_{2.5}$ were also investigated. The correlation of NO_x and PM_{10} was 0.76, and the latter was 0.48. High correlation of NO_x and PM_{10} suggests that PM_{10} level would be strongly associated with traffic emissions and its related activities, while the lower correlation of NO_x and $PM_{2.5}$ implies that most of the emitted PM_{10} was not from the tailpipe. A similar study in China found that the ratios of $PM_{2.5}/PM_{10}$ were 0.617, 0.630, and 0.680 for urban, urban fringe, and suburban³⁹. Munir et al.⁴⁰ presented that the $PM_{2.5}/PM_{10}$ ratio was greater than 0.6 for urban traffic area. Zhao et al.³⁸ suggested that a contribution of more coarse PM sources involved by mechanical processes, e.g. resuspended dust is related to a low ratio of $PM_{2.5}/PM_{10}$ (less than 0.5), whereas a high ratio (greater than 0.6) is related to emissions from industrial and vehicular fuel combustion. In this study, although the air quality monitoring station is located near the road, the ratio of $PM_{2.5}/PM_{10}$ (0.4) does not represent vehicular fuel combustion in the urban area. The high PM_{10} in the area would be affected by mechanical activities more than emission from the traffic tailpipe.

Figure 5 presents the diurnal variations of PM_{10} concentrations and $PM_{2.5}/PM_{10}$ ratios on weekends and weekdays in the selected winter months (November to February). Diurnal changes of PM_{10} for each month expressed the same trend of variations with substantially higher PM_{10} concentrations in January and February

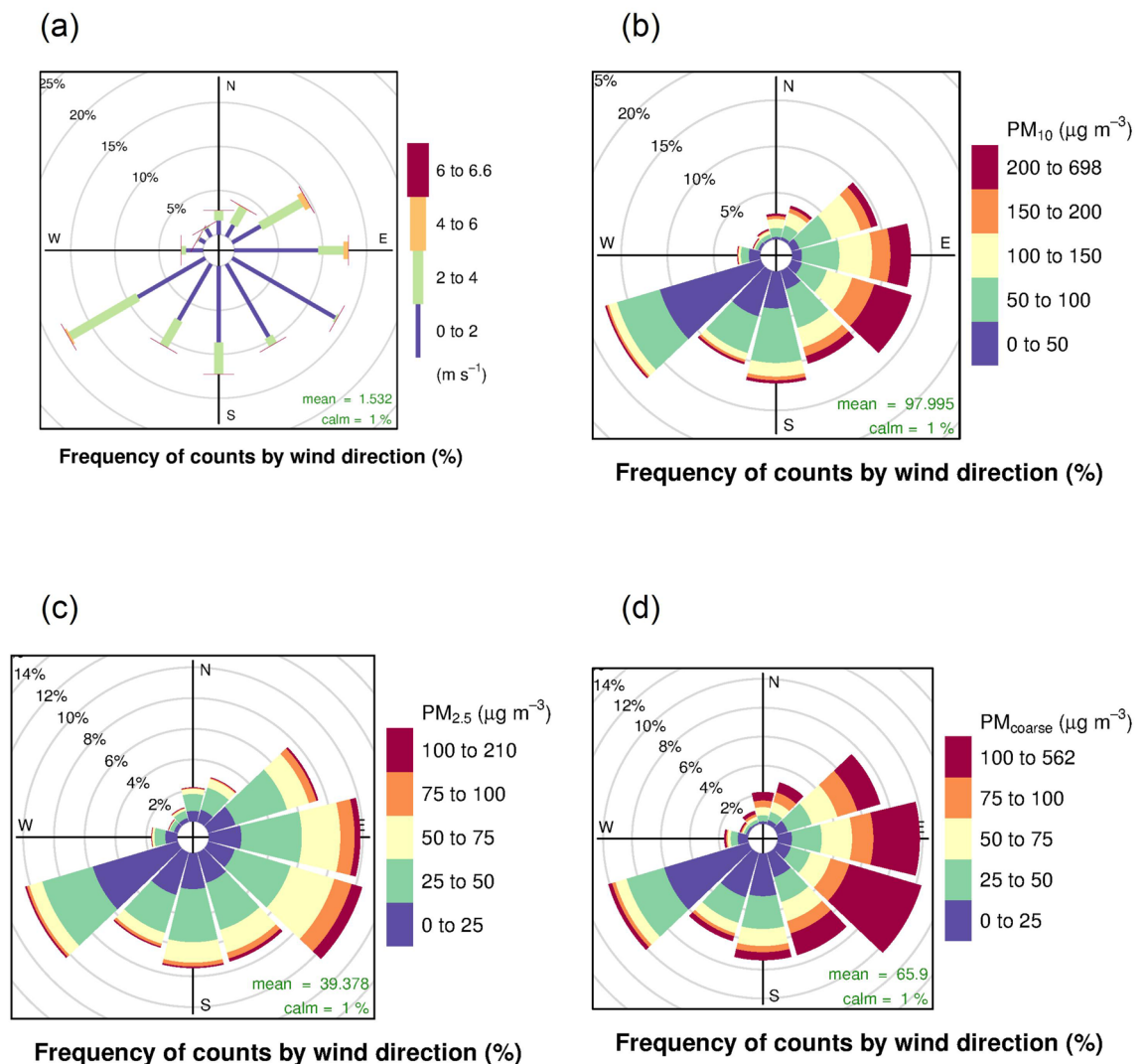


Figure 3. (a) Wind rose and pollution roses of (b) PM_{10} , (c) $PM_{2.5}$, and (d) PM_{coarse} .

than that of the other months (Figure S3 in supplementary). It could be clearly seen that PM_{10} concentrations displayed two peaks daily. The first peak of PM_{10} began to rise at approximately 6:00 until 10:00, and decreased at noon. At around 19:00, PM_{10} concentrations started to rise again until about 23:00 resulting in the second peak observation.

The ratio of $PM_{2.5}/PM_{10}$ rising coincided with PM_{10} reduction such as at 3:00 whereas the ratio reducing coincided with PM_{10} increase such as at 9:00. The change of PM_{10} concentration varied mainly by the change of PM_{coarse} . For other months, they showed the same characteristics, only the proportion of PM_{coarse} changed during the rainy season because large particles were removed from the atmosphere. Notably, the occurrence of the two peaks daily indicated the activities and factors related to the regular emission sources in the area for each day and month. In addition, these two peaks were consistent with Phetrawech and Thepanondh¹⁴ in that the emission rate of resuspended road dust in Na Phra Lan was high from 6:00–9:00 and 19:00–23:00.

Potential sources of PM_{10} . Identifying significant sources of PM_{10} is important for the policymakers to take appropriate action to mitigate and reduce these emissions. Bivariate polar plot technique can be used to identify a significant source^{15,41,42}. The plot uses polar coordinates where the radial axis represents wind speed and the angular axis represents wind direction to display distributing concentrations of PM_{10} around the receptor. When wind speed is low, the mean concentrations will be displayed near the center of the polar coordinate, i.e., the receptor or the air quality monitoring station. However, when wind speed is high, the concentrations will be displayed far from the center. Polar plot results can be interpreted by comparing with the spatial map showing the locations of activities or sources related to PM_{10} emissions in the area.

Figure 6 shows bivariate polar plot analysis based on 4 years of data on air quality and meteorological measurements at Na Phra Lan Subdistrict. High PM_{10} concentrations observed at the air quality monitoring station were identified at two main emission sources (red shading) in the north-east side from November to February. The first potential sources located far from the station corresponding to the low $PM_{2.5}/PM_{10}$ ratios (less than 0.5) (Figure S4 in supplementary). The low ratio was associated with more contribution of primary coarse particles³⁸,

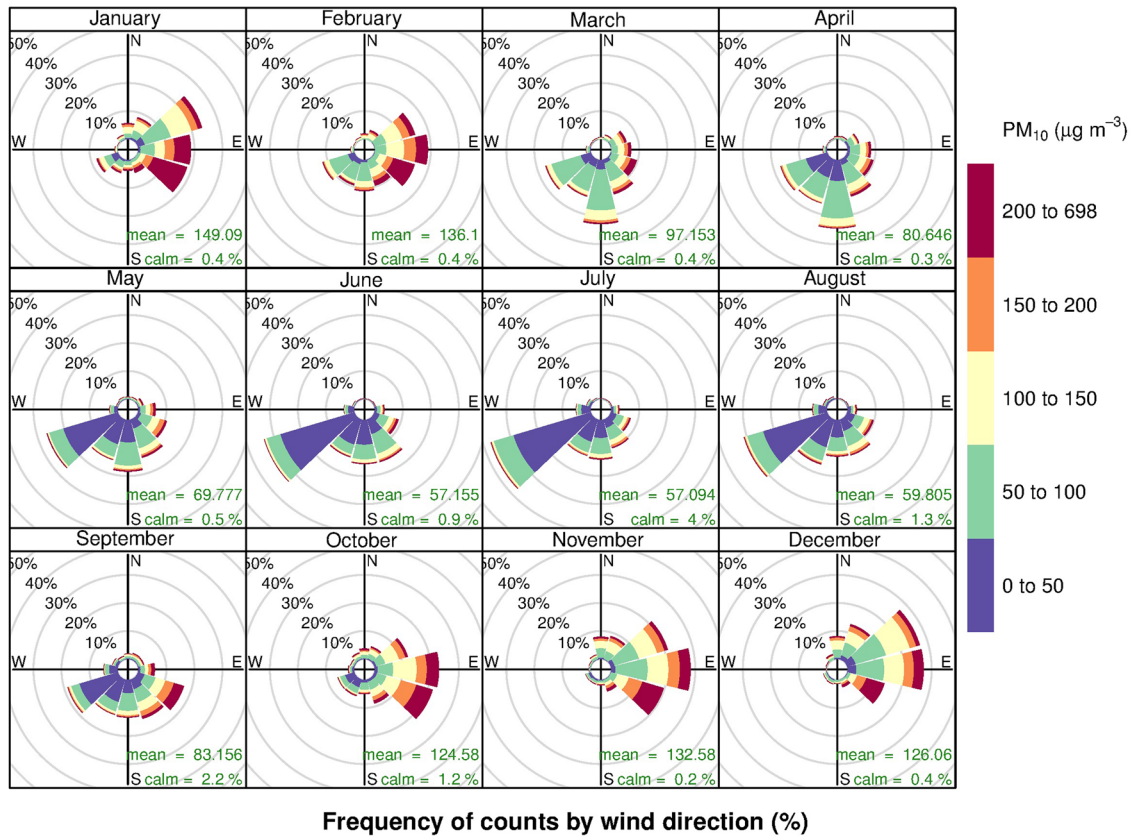


Figure 4. Monthly pollution roses of PM_{10} in Na Phra Lan Subdistrict.

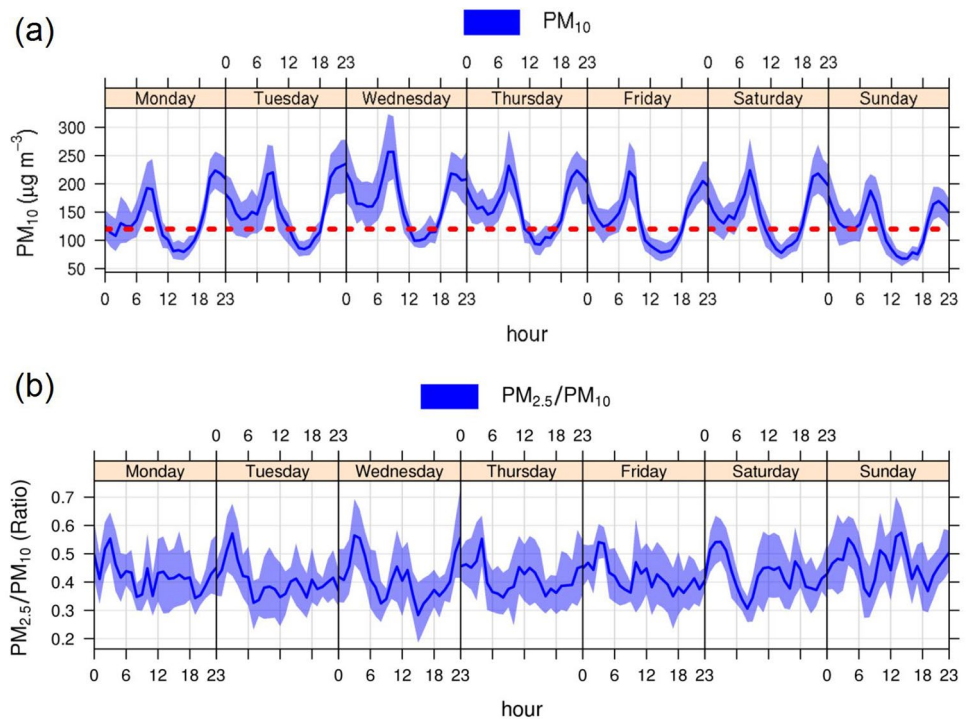


Figure 5. Variation of four year averages of (a) PM_{10} concentrations and (b) $PM_{2.5}/PM_{10}$ ratio on a daily basis in the selected winter months (November to February).

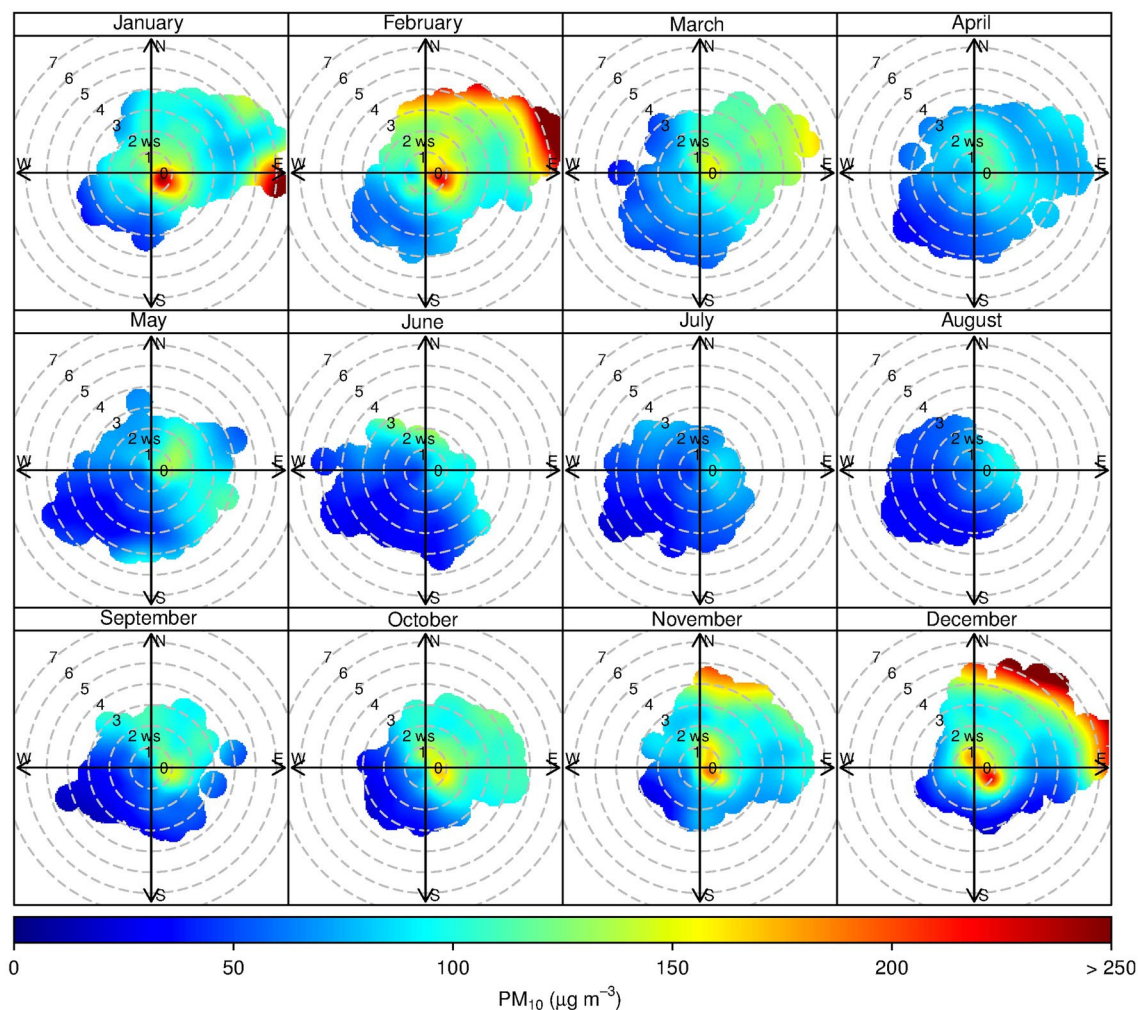


Figure 6. Bivariate polar plot of the mean PM_{10} concentration.

mechanical grinding and crushing activities, and non-combustion sources, such as mining, quarrying, and agriculture⁴⁰. As shown in Fig. 1, the far areas in the north-east side are mining and quarrying activities, which are around 1–5 km from the air quality monitoring station that agrees with this bivariate polar plot analysis results. Not only the far source has small $PM_{2.5}/PM_{10}$ ratio, but the close source is also. The second potential source is present near the air quality monitoring station, which is the roadside and this source is not representative of an urban traffic area. The small $PM_{2.5}/PM_{10}$ ratio would be emitted from soils by wind erosion⁴³ and primary sources related to mechanical processes³⁸. Therefore, the near source would be related to the resuspended road dust from transporting mining products as also suggested by Phetrawech and Thepanondh^{14,44} not tailpipe.

The results obtained from the bivariate polar plot provide information in terms of spatial analysis for source dispersion; however, the polar plot cannot indicate the temporal influence of the source for each time window. Therefore, the CBPF plot was applied to analyse the four years data. The data were divided into four periods: 00:00–05:00, 06:00–10:00, 11:00–18:00, and 19:00–23:00, which were related to the two peaks and diurnal variation of PM_{10} concentration. During the period of diurnal low concentration from late night to morning, 00:00–05:00, the source area located near the air quality monitoring station and the far source in the Northeast direction influenced PM_{10} level (Fig. 7a). The potential source areas of PM_{coarse} were similar to the PM_{10} source areas; but, the potential source area of NO_x presented only the area located near the station. When the first peak of PM_{10} occurred in late morning (06:00–10:00), high PM_{coarse} concentration was found near the monitoring station. At the same time, the emission sources located far from the station started influencing PM_{10} levels (Fig. 7b). At noon (11:00–18:00), the sources located far from the station became the main contributor of PM_{10} at the station during the diurnal low concentration of PM_{10} (Fig. 7c). For the last period, evening to midnight, 19:00–23:00 (Fig. 7d), the second PM_{10} peak period, all PM_{10} , PM_{coarse} , NO_x emission source areas close to the station became the major contributor.

The results indicated that sources close to the air quality station substantially contributed to high concentrations of PM_{10} at the station from night to late morning and contributed to two peak levels of PM_{10} at 06:00–10:00 and 19:00–23:00. However, PM_{10} emission sources located far from the station were the main contributor from 11:00–18:00. The transportation source increased PM_{10} levels from 00:00 to 05:00 and triggered the first PM_{10}

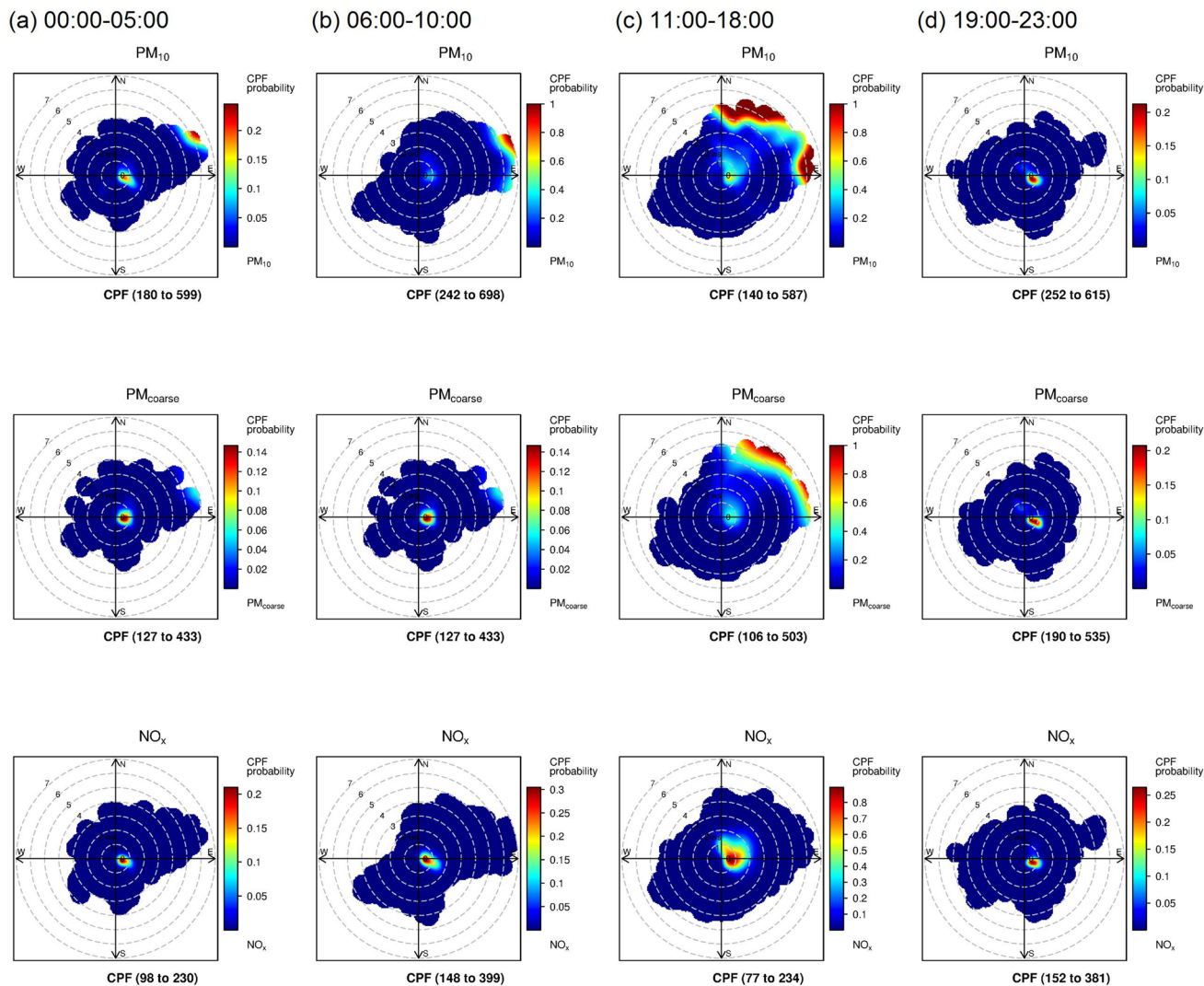


Figure 7. CBPF plot of PM₁₀, PM_{coarse}, NO_x concentrations for 91–100 percentile range at four periods (a) 00:00–05:00, (b) 06:00–10:00, (c) 11:00–18:00, (d) 19:00–23:00. (Range in the bracket is the concentration range in a unit of μg/m³ and ppb for PM and NO_x, respectively).

peak from 06:00–10:00. The increased PM₁₀ was mostly contributed by PM_{coarse}, which would be from the resuspended dust caused by transportation and the wind blowing from the mining and quarrying areas. The influence of mining and quarrying industries started contributing to PM₁₀ level and became the main contributor of PM₁₀ after 11:00 until 18:00. The increased level of PM₁₀ at the air quality station during day time was affected by the dispersion from mining and quarrying areas to the station¹³. From 19:00–23:00, the second PM₁₀ peak occurred, the main source being the transportation sector. The PM₁₀ level in the second peak was mostly higher than the level of the first peak. The reason could be due to the stable condition of atmosphere and the reduced mixing layer height during the nocturnal time period resulting in limited vertical dispersion¹³. This mechanism of source emission and meteorology repeated on the next day and month.

This finding confirmed that the street located close to the station was an important source to trigger and increase the PM₁₀ level by the resuspended dust more than emission of tailpipe from daybreak to late morning that resulted in PM₁₀ peaks. The distant source from the industrial processes of mining and stone crushing in the north-east side maintained the background PM₁₀ concentration in the area.

Conclusion

The PM, NO_x and meteorological data observed at the air quality monitoring station located in Na Phra Lan Subdistrict, Saraburi Province, Thailand for the past four years were analysed to understand the air quality situation and characterise PM₁₀ emission sources. From time series analysis, the mean concentration of PM₁₀ in Na Phra Lan Subdistrict was higher than the NAAQS of Thailand and interim target-2 level of WHO mainly from October-February. The small PM_{2.5}/PM₁₀ ratio suggests that high PM₁₀ concentration is caused more by PM_{coarse} than PM_{2.5}, and related to primary sources, mining, and quarrying. The diurnal variation of hourly PM₁₀ concentrations revealed two peak periods from 06:00–10:00 and 19:00–23:00 daily and monthly. This

means PM₁₀ levels exhibited similar daily behaviours contributed from the constant source emissions. Using bivariate polar plot and CBPF, the first potential source areas of PM₁₀ were found at the far area in the northeast side. Most activities in this area were related to stone crushing, quarrying and mining industries. The second potential source was an area adjacent to the air quality monitoring station, in the area of the street. The small PM_{2.5}/PM₁₀ ratio presented over the near-source area implies less PM_{2.5}; thus, the main source would be related to resuspended dust rather than the tailpipe emissions. Both of potential source areas played an important role in establishing the first PM₁₀ peak. After that, the PM₁₀ concentration decreased during the 11:00–18:00 and the far source area became the potential source. The near-source area, later on, contributed significantly in increasing PM₁₀ by traffic acting to spread coarse dust in the later time during the nocturnal condition. The analysis with time series and CBPF could identify the mechanism and source that affected high PM₁₀ concentration range in the specific location and temporal variations. From this study, we concluded that the industrial source of mining, stone crushing, and quarrying area played a role regarding background PM₁₀ concentrations in Na Phra Lan Subdistrict and the mobile source was a factor to rebound PM₁₀, particularly PM_{coarse}, from the road to ambient air resulting in two PM₁₀ peaks daily. To overcome the nonattainment area for PM₁₀ attributable to the mining industrial and relating processes, we proposed that countermeasure activities, e.g., road cleaning before the peak times, change the route for transporting products from the mine and quarry, and improvement of industrial processes at the potential source area, particularly during October to February, would be required to reduce background PM₁₀ levels.

Received: 30 March 2020; Accepted: 25 November 2020

Published online: 07 December 2020

References

1. UNSD. *Sustainable development goal (SDG) indicators correspondence with the basic set of environment statistics of the FDES 2013* (United Nations Statistics Division, New York, 2018).
2. WHO. *WHO air quality guidelines for particulate matter, ozone, nitrogen dioxide and sulfur dioxide (global update 2005)* (WHO Press, 2006).
3. Landrigan, P. J. *et al.* The lancet commission on pollution and health. *Lancet Commis.* **91**, 462–512 (2018).
4. Maji, K. J., Arora, M. & Dikshit, A. K. Burden of disease attributed to ambient PM_{2.5} and PM₁₀ exposure in 190 cities in China. *Environ. Sci. Pollut. Res.* **24**, 11559–11572 (2017).
5. Liao, Z., Sun, J., Liu, J., Guo, S. & Fan, S. Long-term trends in ambient particulate matter, chemical composition, and associated health risk and mortality burden in Hong Kong (1995–2016). *Air Qual. Atmos. Health* **11**, 773–783 (2018).
6. Bowe, B. *et al.* The 2016 global and national burden of diabetes mellitus attributable to PM_{2.5} air pollution. *Lancet Planetary Health*. **2**, e301–e312 (2018).
7. Kassomenos, P. A., Dimitriou, K. & Paschalidou, A. K. Human health damage caused by particulate matter PM₁₀ and ozone in urban environments: The case of Athens Greece. *Environ. Monit. Assess.* **185**, 6933–6942 (2013).
8. WHO. *Ambient Air pollution: a global assessment of exposure and burden of disease* (WHO Press, 2016)
9. Taneepanichskul, N. *et al.* Short-term effects of particulate matter exposure on daily mortality in Thailand: A case-crossover study. *Air Qual. Atmos. Health* **11**, 639–647 (2018).
10. PCD. *Thailand's state of pollution report 2017* (Pollution Control Department, 2018).
11. National Environmental Board. *Notification of National Environmental Board No. 23, B.E. 2547 (2004)* (National Environmental Board, 2004).
12. Pimonsree, S., Wongwises, P., Pan-Aram, R. & Zhang, M. Spatial and temporal variations of PM₁₀ concentrations over a mineral products industrial area in Saraburi. *KMUTT Res. Dev. J.* **32**, 355–371 (2009).
13. Pimonsree, S., Wongwises, P., Pan-Aram, R. & Zhang, M. Model analysis of PM₁₀ concentration variations over a mineral products industrial area in Saraburi, Thailand. *Water Air Soil Pollut.* **201**, 239–251 (2009).
14. Phetravech, T. & Thepanondh, S. Source contributions of PM-10 concentrations in the Na PhraLan Pollution Control Zone, Saraburi Thailand. *Sci. Technol. Asia.* **22**, 60–70 (2017).
15. Uria-Tellaetxe, I. & Carslaw, D. C. Conditional bivariate probability function for source identification. *Environ. Model. Softw.* **59**, 1–9 (2014).
16. Bang, H. Q., Ngoc Khue, V. H., Tam, N. T. & Lasko, K. Air pollution emission inventory and air quality modeling for Can Tho City, Mekong Delta, Vietnam. *Air Qual. Atmos. Health.* **11**, 35–47 (2018).
17. Malby, A. R., Whyatt, J. D. & Timmis, R. J. Conditional extraction of air-pollutant source signals from air-quality monitoring. *Atmos. Environ.* **74**, 112–122 (2013).
18. Mukherjee, A., Agrawal, S. B. & Agrawal, M. Intra-urban variability of ozone in a tropical city-characterization of local and regional sources and major influencing factors. *Air Qual. Atmos. Health* **11**, 965–977 (2018).
19. Garza-Galindo, R. *et al.* Spatial and temporal distribution of metals in PM_{2.5} during 2013: Assessment of wind patterns to the impacts of geogenic and anthropogenic sources. *Environ. Monit. Assess.* **191**, 165 (2019).
20. Bae, M. S. *et al.* Identifying pollutant source directions using multiple analysis methods at a rural location in New York. *Atmos. Environ.* **45**, 2531–2540 (2011).
21. Perišić, M. *et al.* Estimation of required PM₁₀ emission source reduction on the basis of a 10-year period data. *Air Qual. Atmos. Health* **8**, 379–389 (2015).
22. Khanum, F., Chaudhry, M. N. & Kumar, P. Characterization of five-year observation data of fine particulate matter in the metropolitan area of Lahore. *Air Qual. Atmos. Health* **10**, 725–736 (2017).
23. Molina, C., Toro, R. A., Morales, R. G. E. S., Manzano, C. & Leiva-Guzmán, M. A. Particulate matter in urban areas of south-central Chile exceeds air quality standards. *Air Qual. Atmos. Health* **10**, 653–667 (2017).
24. R Core Team. A language and environment for statistical computing. <http://www.R-project.org/> (2013).
25. Carslaw, D. C. & Ropkins, K. Openair—An R package for air quality data analysis. *Environ. Model. Softw.* **27–28**, 52–61 (2012).
26. Szulecka, A., Oleniacz, R. & Rzeszutek, M. Functionality of openair package in air pollution assessment and modeling—a case study of Krakow. *Environ. Protect. Nat. Resour.* **28**, 22–27 (2017).
27. Bennett, N. D. *et al.* Characterising performance of environmental models. *Environ. Model. Softw.* **40**, 1–20 (2013).
28. Sooktawe, S., Humphries, U., Limsakul, A. & Wongwises, P. Spatio-temporal variability of winter monsoon over the Indochina Peninsula. *Atmosphere.* **5**, 101–121 (2014).
29. Khamkaew, C. *et al.* Investigation of biomass burning chemical components over northern Southeast Asia during 7-SEAS/baseline 2014 campaign. *Aerosol Air Qual. Res.* **16**, 655–2670 (2016).

30. Ha, K. J. *et al.* Variability in the East Asian Monsoon: A review. *Meteorol. Appl.* **19**, 200–215 (2012).
31. McGrath-Spangler, E. L. & Denning, A. S. Global seasonal variations of midday planetary boundary layer depth from CALIPSO space-borne LIDAR. *J. Geophys. Res. Atmos.* **118**, 1226–1233 (2013).
32. Feng, X., Wu, B. & Yan, N. A method for deriving the boundary layer mixing height from MODIS atmospheric profile data. *Atmosphere*. **6**, 1346–1361 (2015).
33. Limsakul, A., Limjirakan, S. & Suttamanuswong, B. Asian summer monsoon and its associated rainfall variability in Thailand. *Environ. Asia*. **3**, 79–89 (2010).
34. Kim, S. *et al.* Effect of precipitation on air pollutant concentration in Seoul Korea. *Asian J. Atmos. Environ.* **8**, 202–211 (2014).
35. Kim Oanh, N. T., Chutimon, P., Ekbordin, W. & Supat, W. Meteorological pattern classification and application for forecasting air pollution episode potential in a mountain-valley area. *Atmos. Environ.* **39**, 1211–1225 (2005).
36. Kim Oanh, N. T. & Leelasakultum, K. Analysis of meteorology and emission in haze episode prevalence over mountain-bounded region for early warning. *Sci. Total Environ.* **409**, 2261–2271 (2011).
37. Thepnuan, D., Chantara, S., Lee, C. T., Lin, N. H. & Tsai, Y. I. Molecular markers for biomass burning associated with the characterization of PM_{2.5} and component sources during dry season haze episodes in Upper South East Asia. *Sci. Total Environ.* **658**, 708–722 (2019).
38. Zhao, D., Chen, H., Yu, E. & Luo, T. PM_{2.5}/PM₁₀ ratios in eight economic regions and their relationship with meteorology in China. *Adv. Meteorol.* **2**, 1–15 (2019).
39. Xu, G. *et al.* Spatial and temporal variability of the PM_{2.5}/PM₁₀ ratio in Wuhan, Central China. *Aerosol Air Qual. Res.* **17**, 741–751 (2017).
40. Munir, S. Analysing temporal trends in the ratios of PM_{2.5}/PM₁₀ in the UK. *Aerosol Air Qual. Res.* **17**, 34–48 (2017).
41. Hayes, E. T., Chatterton, T. J., Barnes, J. H. & Longhurst, J. W. S. Utilising openair to support multi-stakeholder engagement and the resolution of air quality issues. *Clean Air J.* **23**, 23–31 (2013).
42. Silva, J. *et al.* Particulate matter levels in a South American megacity: The metropolitan area of Lima-Callao Peru. *Environ. Monit. Assess.* **189**, 635 (2017).
43. Li, H., Tatarko, J., Kucharski, M. & Dong, Z. PM_{2.5} and PM₁₀ emissions from agricultural soils by wind erosion. *Aeolian Res.* **19**, 171–182 (2015).
44. Phetrawech, T. & Thepanondh, S. Evaluation of resuspension of road dust in a cement industrial complex area. *Int. J. GEOMATE.* **12**, 96–103 (2017).

Acknowledgements

The authors express their thanks to the Pollution Control Department for data support and the developers of the R software and OpenAir package for the tools used in this study.

Author contributions

S.S. and T.K. designed and developed the study. S.B., A.P., N.P. collected and analysed the data. S.S. and T.K. interpreted the results and wrote the manuscript.

Competing interests

The authors declare no competing interests.

Additional information

Supplementary Information The online version contains supplementary material available at <https://doi.org/10.1038/s41598-020-78445-5>.

Correspondence and requests for materials should be addressed to T.K.

Reprints and permissions information is available at www.nature.com/reprints.

Publisher's note Springer Nature remains neutral with regard to jurisdictional claims in published maps and institutional affiliations.



Open Access This article is licensed under a Creative Commons Attribution 4.0 International License, which permits use, sharing, adaptation, distribution and reproduction in any medium or format, as long as you give appropriate credit to the original author(s) and the source, provide a link to the Creative Commons licence, and indicate if changes were made. The images or other third party material in this article are included in the article's Creative Commons licence, unless indicated otherwise in a credit line to the material. If material is not included in the article's Creative Commons licence and your intended use is not permitted by statutory regulation or exceeds the permitted use, you will need to obtain permission directly from the copyright holder. To view a copy of this licence, visit <http://creativecommons.org/licenses/by/4.0/>.

© The Author(s) 2020